Energy 90 (2015) 1024–1032

Contents lists available at ScienceDirect

Energy

journal homepage: www.elsevier.com/locate/energy

Performance evaluation of various cryogenic energy storage systems

Rodrigo F. Abdo [a], Hugo T.C. Pedro [b], Ricardo N.N. Koury [a], Luiz Machado [a], Carlos F.M. Coimbra [b], Matheus P. Porto [a, *]

[a] Grupo de Energias Renováveis, Laboratório de Termometria, LabTerm, Programa de Pós Graduação em Engenharia Mecânica PPGMEC, Escola de Engenharia da Universidade Federal de Minas Gerais, Belo Horizonte, MG, Brazil
[b] Department of Mechanical and Aerospace Engineering, Jacobs School of Engineering, and Center for Energy Research, University of California San Diego, La Jolla, CA, USA

ARTICLE INFO

Article history:
Received 14 April 2015
Received in revised form
9 July 2015
Accepted 6 August 2015
Available online 28 August 2015

Keywords:
Cryogenic energy storage
Liquid air energy storage
Cogeneration
Renewable energy

ABSTRACT

This work compares various CES (cryogenic energy storage) systems as possible candidates to store energy from renewable sources. Mitigating solar and wind power variability and its direct effect on local grid stability are already a substantial technological bottleneck for increasing market penetration of these technologies. In this context, CES systems represent low-cost solutions for variability that can be used to set critical power ramp rates. We investigate the different thermodynamic and engineering constraints that affect the design of CES systems, presenting theoretical simulations, indicating that optimization is also needed to improve the cryogenic plant performance.

1. Introduction

Exergy gives the maximum potential of a renewable source to generate work, and different methods to evaluate the natural exergy have been discussed by several authors [1–5]. The flow availability (α) of natural sources, in a reversible process, can be evaluated by Eq. (1) that quantifies the specific exergy in an arbitrary point.

$$\alpha = \left(h - T_0 s + \frac{1}{2}V^2 + gZ\right) - (h_0 - T_0 s_0 + gZ_0), \tag{1}$$

where h is the specific enthalpy, T is the absolute temperature, s is the specific entropy, V is the velocity, Z is the elevation, g is the gravity, and subscript 0 refers to the dead state and the arbitrary elevation reference. For example, wind speed natural availability can be approximated by $\frac{1}{2}V^2$, and potential energy from reservoirs can be approximated by $g(z - z_0)$. This flow availability can be converted into useful forms of energy, for example by converting it into angular-momentum using turbines which is later converted into electric energy at the cost of new irreversibilities. During these processes, the total extracted work (W) is obtained from the exergy balance equation, Eq. (2).

$$W = (\alpha_1 - \alpha_2) - I, \tag{2}$$

where I represents the process irreversibility, the difference $\alpha_1 - \alpha_2$ is the availability (maximum work) between thermodynamic states 1 and 2, respectively. Eventually electric energy is transmitted to the grid line or transferred to energy storage devices. The purpose of energy storage is to transform part of the converted availability (see Eq. (1)) in to an ordered (manageable) form of energy conversion. This type of technology has been targeted as one of the solutions to enable higher penetration of volatile renewable resources, such as solar and wind, into the power grid [6].

One of the devices used to recover this availability is the LAES (liquid air energy storage), also called CES (cryogenic energy storage). The first CES system dates from 1900 [7], when the Tripler Liquid Air Company designed a liquid–air fueled car for competing with the steam and electric vehicles of those days. During the oil crisis in the 1970s, the interest in cryogenic cars returned. At the same time emerged the interest of using air liquefaction as an energy storage system [8].

In the literature [9,10], the term CES [7], or LAES, generally is used to refer to energy storage of liquefied air. Currently, hydrogen and air/nitrogen are two of the most promising alternatives of CES

* Corresponding author.
E-mail address: matheusporto@ufmg.br (M.P. Porto).

http://dx.doi.org/10.1016/j.energy.2015.08.008
0360-5442/

Nomenclature

E	exergy, kW
g	gravity, m s^{-2}
h	enthalpy, kJ kg^{-1}
I	irreversibility, kJ kg^{-1}
k	specific heat ratio
L	conditional parameter of Eqs. (6) and (7)
m	mass, kg
MFR	mass flow ratio, $\dot{m}_{exp}/\dot{m}_{liq}$
n	conditional parameter of Eqs. (6) and (7)
$\dot{m}$	mass flow rate, kg s^{-1}
P	pressure, Pa
q	quality
R	universal gas constant, kJ kg^{-1} K^{-1}
s	entropy, kJ kg^{-1} K^{-1}
t	time, s
T	temperature, K
U	internal energy, kJ/kg
V	velocity, m s^{-1}
v	specific volume, m^3/kg
W	work, kJ
$\dot{W}$	power, kW
x	proportion of liquid produced
z	proportion of bypassed mass flow
Z	height, m

Greek

α	flow availability, kJ kg^{-1}
ε	effectiveness
γ	proportion of saturated vapor inside the tank
η	process efficiency
ρ	density, kg/m^3
ψ	overall efficiency

Subscripts

0	dead state
a,b,c,d,e	geometric position in Fig. 1
bpt	bypass turbine
cla	Claude cycle
col	Collins cycle
exp	expansion circuit
ht	heat exchanger
i	inlet
ie	isentropic
iso	isothermal
l	saturated liquid
lin	Linde–Hampson cycle
liq	liquefaction circuit
o	outlet
p	pump
st	storage
t	turbine
v	saturated vapor

working fluids [11,9]. However, Li et al. [9] compared hydrogen and air/nitrogen for energy storage, concluding that even with similar efficiency liquefied air is more competitive as an energy carrier in terms of capital costs. Recently, Akhusrst [7] published a report regarding the use of liquid–air in the energy and transport systems, indicating the important potential of CES for those applications. In terms of CES applications Li et al. [12] proposed a combination of nuclear power plants and CES for load shifting at peak hours. The same authors proposed a new hybrid system comprised of a solar thermal plant and a cryogen fueled power system [13], indicating that this approach provides more power than the summation of the two systems working separately. Zhang et al. [14] assessed the operational benefits of using CES in an existing air separation plant, looking for new potential opportunities of the technology, as load shifting by storing purchased energy and selling it back during higher-price periods, thus creating additional revenues. When applied to a real-world industrial plant, authors concluded that CES can be very attractive, mainly for underutilized air separation plants. According to Hadi and Zadeh [15], the relatively high energy density and high efficiency of energy conversion, make CES a singular method for energy storage. Chen et al. [16] highlight that CES is a low-footprint technology, and can be also used to provide cooling and refrigeration. Hadi [15] presented an investigation of the economic viability and profitability of CES systems. Li et al. [17] presented a critical assessment on cryogen as an energy carrier, highlighting that direct expansion combined with a Rankine cycle is promising when carbon dioxide capture is used, as detailed in Ref. [18]. Despite the importance of CO_2 capturing [19,20] and cascading cycles [21–23], the work here presented gives attention to the liquid air physical exergy in a direct expansion process.

The overall efficiency of liquid air production ranges between 11% and 50%, depending on the plant size [9]. After the liquefaction process, the availability of the liquid air is used to produce electricity. This conversion has a large potential for loosing energy to atmosphere due to the cryogenic temperature resulting in a lower efficiency (up to 40%). Looking for a higher efficiency, Chen et al. [10] patented a cycle to recover this physical exergy, producing liquid air at the same time as air is expanded and electricity is produced (this process is better explained in the following section). The novel solution of CES, conceived by Chen et al. [10], is based on Linde–Hampson cycle. Ameel et al. [24] simulated the cycle proposed by Chen et al. and concluded that it is very sensitive to the efficiency of the heat exchanger, compressor and turbine. The authors concluded that this cycle reaches a maximum efficiency of 43.3% without using any external source of energy, and 63.7% considering an isothermal expansion at 400 K.

In this work we evaluate again the solution proposed by Chen et al. [10], and introduce other alternatives based on Claude and Collins cycles. The presented solutions can reach higher values of efficiency, when compared to the Chen et al. [10] approach, as demonstrated in the following sections.

2. Methodology

This section was divided in two subsections. Aspects related to the liquefaction process are shown in the first part of this section. In the second part, a discussion on the expansion circuit is presented.

2.1. Liquefaction circuit

The purpose of the liquefaction circuit is to produce liquid nitrogen from atmospheric air. Industrial production of liquid nitrogen began in England, France and Germany in 1902, pioneered by Willian Hampson, Carl Linde, Georges Claude, and Charles Tripler [25]. Linde patented his cycle in 1903 [26], which is considered the simplest approach to produce liquid from gases (see ref. [27]), but it

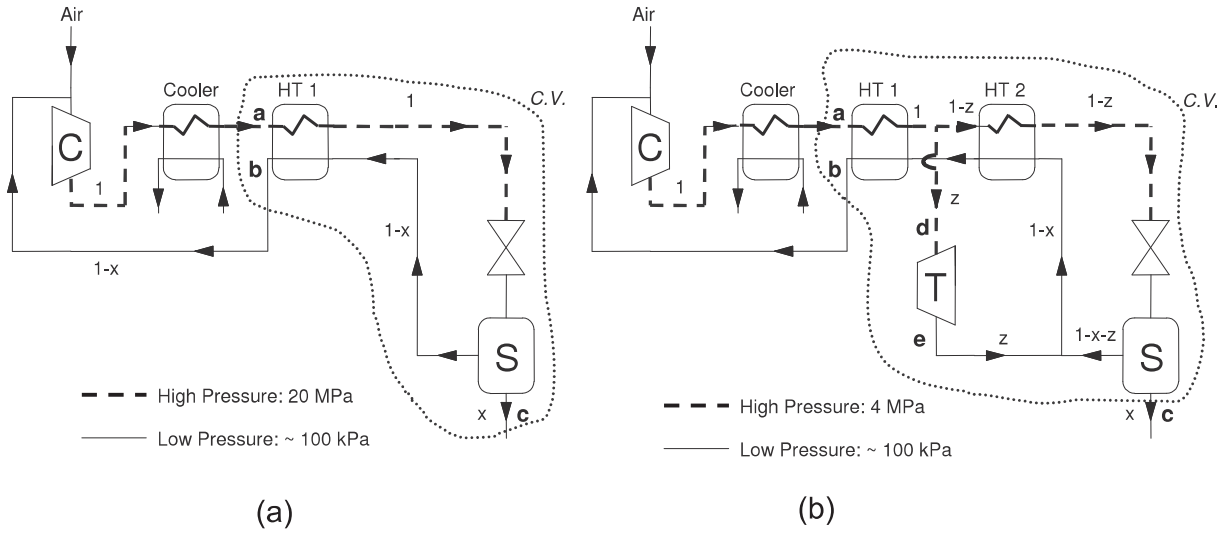

Fig. 1. (a) Schematic view of Linde–Hampson and (b) Claude liquefaction system; (C = compressor, T = turbine, HT = heat exchanger, S = storage tank).

is not the easiest to operate because high pressures are involved (20 MPa are required at the high pressure line), see Fig. 1(a). Additionally this cycle yields a low relative rate of liquid production. This value for Linde–Hampson cycle (x_{lin}) can be determined by Eq. (3).

$$x_{lin} = \frac{\dot{m}_l}{\dot{m}_i} = \left[\frac{h_a - h_b}{h_c - h_b}\right], \tag{3}$$

where x represents the proportion of liquid produced ($\dot{m}_i$) from the compressor's total mass flow rate ($\dot{m}_l$), and h is the specific enthalpy for each point depicted in Fig. 1(a). Eq. (3) is obtained from the energy balance of the control volume depicted in Fig. 1(a), when all processes involved are considered adiabatic.

Seeking to develop a cycle with lower working pressures, Claude proposed a solution with two expansion mechanisms, a Joule–Thomson effect valve and a turbine (which is located along a bypass, after the first heat exchanger, see Fig. 1(b). It can be shown that, using the control volume presented in Fig. 1, the proportion of the compressor mass flow turned into liquid for the Claude cycle (x_{cla}) is expressed by

$$x_{cla} = \frac{h_a - h_b}{h_c - h_b} + z\frac{h_d - h_e}{h_c - h_b}, \tag{4}$$

where z is the ratio of the by-passed mass flow rate and compressor mass flow rate, and h is the specific enthalpy for each point indicated in Fig. 1(b). Considering a compressor output pressure equal to 4 MPa, z = 80% (arbitrarily chosen), and the control volume depicted in Fig. 1(b), it is possible to determine the proportion of the compressor mass flow that is liquefied, which is equal to 14.5%. For the same $h_c - h_b$, the Linde–Hampson system operating at higher pressure (20 MPa) yields 6.5% of liquefied air. Considering that there is no totally adiabatic system at these cryogenic temperatures, and assuming a realistic heat exchanger efficiency of 80%, the rate of liquid production for the Claude system decreases to 7.1%. This value can be improved using the Collins Cycle, which uses the same concept as presented by Claude, but more turbines are included in parallel. For this case the relative production of liquid rate (x_{col}) is given by Eq. (5).

$$x_{col} = \frac{h_a - h_b}{h_c - h_b} + \sum_i z_i \frac{\Delta h_i}{h_c - h_b}. \tag{5}$$

where i denotes the number of turbines (and bypasses) present in the cycle, and Δh represents the work obtained from each turbine. If $i = 1$, Collins system will have the same configuration as Claude system, and if $z = 0$ (turbines are not considered) the Claude system is converted into a Linde–Hampson system. Using Collins cycle, the pressure can be even lower than the ones for the Claude cycle, and liquid production can be higher. Other authors as Valenti [28] have presented more efficient cycles based on the same components as exposed here.

2.2. Expansion circuit

Fig. 2(a) shows the basic form of a CES recovering system. In this scheme, liquefied air, provided from an external source, is reclaimed from a tank and pumped into the turbine using a cryogenic pump. During this process a large amount of energy is lost to the surroundings by the air heat exchanger, limiting the overall efficiency to about 40%.

Looking to improve this system, Li et al. [17] proposed a combined system using CES and an expansion-Rankine cycle with propane, as shown in Fig. 2(b). In this method the “cold” energy is not lost to the atmosphere as in the CES basic form. Instead it is transferred by the heat exchanger to the propane circuit, and recovered through a turbine. Under ideal conditions the exergetic efficiency of this system can reach 78%. Another approach for taking advantage of the “cold” energy from the cryogenic tank was patented by Chen et al. [10] (Fig. 2(c)). In this design, at the same time that liquefied air is sent by a cryogenic pump from the tank to the turbine (expansion circuit), ambient air is sent back, in a smaller proportion, to the tank using a compressor. The compressed air passes through a heat exchanger to receive “cold” energy from the “expansion circuit” side, then expands and liquefies through an expansion valve (Joule–Thomson valve) and is stored into the tank (liquefaction circuit). If an external thermal source is used in the expansion circuit (heated water from a solar heater and/or compression process TES) the efficiency can reach 63% [24].

The CES solutions presented in Fig. 2(c) and (d) combine cold-TES and hot-TES tanks, as thermal storage alternatives. The cold-

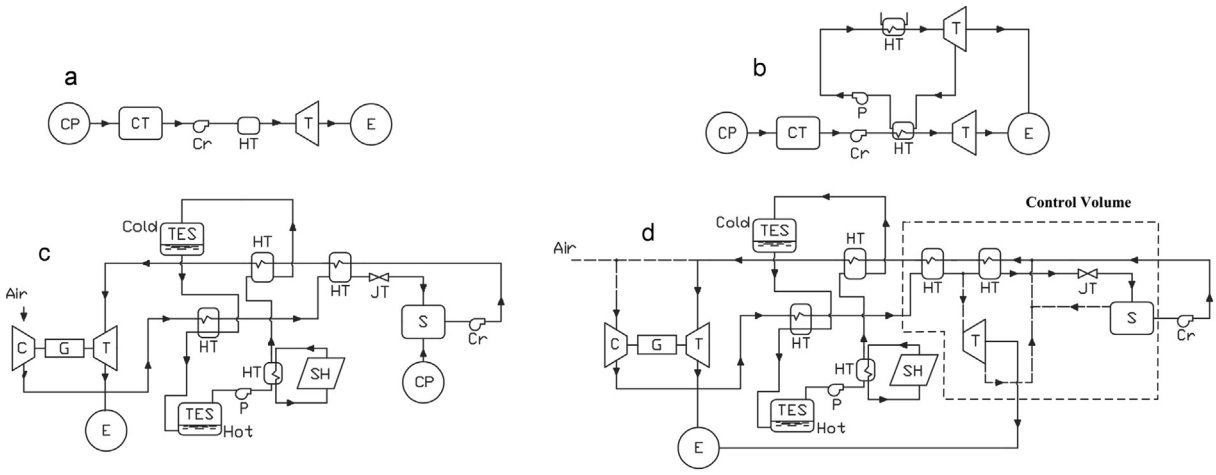

Fig. 2. Schematic view of different CES applied for renewable sources of energy (C = compressor, CP = cryogenic plant, CT = cryogenic tank, E = electrical grid, G = generator, T = turbine, HT = heat exchanger, TES = thermal energy storage, S = storage tank, P = pump, SH = solar heater, Cr = Cryogenic Pump, JT = Joule Thomson valve, dashed line = used if liquefaction is the only current process); (a) basic CES, (b) CES/expansion-Rankine-propane cycle, (c) CES-Linde–Hampson with recovering system [10], (d) CES-Claude with recovering system.

TES of Fig. 2(d) could be a simple static water tank, for example, that operates close to the ambient temperature. The secondary fluid (Therminol, for example) receives thermal energy from the heated air coming from the compressor, by means of a heat exchanger increasing its temperature. This absorbed energy is stored in the hot-TES, using concrete modulus or a phase change material for example. After, the secondary fluid exchanges thermal energy with a circuit of solar thermal collectors increasing its temperature (the thermal solar system also has a hot-TES tank, which is not represented here). The thermal energy from the secondary fluid will then be transferred to the expansion circuit (which has air at high pressure, but low temperature, close to the ambient temperature). As a consequence, the secondary fluid cools down and is used to maintain the cold-TES temperature close to the ambient temperature.

Despite the fact that Chen's plant may also work as a liquefaction plant, it may not actually accumulate liquid air. If liquefaction and expansion circuits work simultaneously there is net production of liquid if the mass flow rate of liquid produced is higher than the one consumed by the expansion circuit. If the reverse happens there is no net production of liquid. If liquefaction and expansion circuits work alternately liquid will be accumulated during liquefaction and consumed during the expansion. A similar analysis can be made for the power output. If the circuits work simultaneously, there will be power output or consumption, depending on the mass flow rate of each circuit. In case of liquefaction only, there will always be power consumption, but in case of expansion only, there will always be power output.

The liquefaction process used in this method is the Linde–Hampson [29], and CES systems that use this process are referred to as CES-Linde–Hampson systems. As the Linde–Hampson process is the simplest and most inefficient liquefaction process, better results can be obtained using Claude cycle. Fig. 2(d) presents a CES-Claude approach. This approach is used in this work as a self sufficient system since it also produces liquefied air: when the cycle works just as a liquefaction plant, the part of the circuit enclosed by the dashed line (see Fig. 2(d)) is activated, turning the system into a Claude liquefaction plant. The discharging system is comprised of a pump, which delivers cryogenic fluid at high pressure to the heat exchanger (where it becomes vapor); afterwards, the high pressure vapor undergoes an expansion in the turbine generating power. Since the mass flow rate is constant, the power delivered by the turbine is also constant.

3. CES modeling

In this section we present a methodology to evaluate the performance of CES-Linde–Hampson, CES-Claude and CES-Collins based on the approach of Fig. 2(d).

We used the concepts described in the previous section to present the relations to the efficiency ψ (see Eq. (6)), and the liquefaction rate x (see Eq. (7)), of the CES systems: CES-Linde–Hampson, CES-Claude and CES-Collins.

$$\psi = \frac{\text{Output power}}{\text{Input power}} = \frac{\sum_{i=1}^{n_t} \dot{W}_{t,i}}{\dot{W}_c + \dot{W}_p}, \tag{6}$$

$$x = \begin{cases} \dfrac{[(h_b - h_a) - (1-\varepsilon)(h_b - h_v)] + MFR.h_l + \dfrac{1}{\dot{m}_{liq}}\dfrac{dU}{dt} + \gamma h_b}{h_b - (1-\varepsilon)(h_b - h_v)} + \displaystyle\sum_{k=1}^{n_t} z_k \eta_{t,k} \frac{(h_{d,k} - h_{e,k})}{h_b - (1-\varepsilon)(h_b - h_v)} & \text{if} \quad MFR + \displaystyle\sum_{i=1}^{n_t} z_i < 1 - \frac{1}{\dot{m}_{liq}}\frac{d\dot{m}}{dt} \\ 0.99 - \displaystyle\sum_{i=1}^{t} z_i & \text{otherwise} \end{cases} \tag{7}$$

where

$$\frac{dU}{dt} = \left(x\dot{m}_{liq} - \dot{m}_{exp}\right)(h_l - h_v\rho_v v_l) \tag{8}$$

$$\gamma = \rho_v v_l (x - MFR) \tag{9}$$

$$\frac{dm}{dt} = \left(x\dot{m}_{liq} - \dot{m}_{exp}\right)(1 - \rho_v v_l) \tag{10}$$

where subscripts a, b, c, d and e are points shown in Fig. 1 at the CES circuit, and $n_t = 0$ (Linde–Hampson cycle), 1 (Claude cycle), or 2 (Collins cycle).

Equation (6) was obtained from the control volume covering all CES system and quantifies the efficiency considering also the savings due to cogeneration for the liquefaction and expansion circuit working simultaneously, where $\dot{W}_c, \dot{W}_p$ and $\dot{W}_t$ are the work done by the compressor, cryogenic pump and turbine, respectively. Equation (7) was obtained considering the control volume shown in Fig. 2(d), which includes the heat exchangers of the expansion-liquefaction circuit, the bypass turbines, Joule–Thomson valve and cryogenic tank. In this equation ε is the effectiveness, MFR is the mass flow ratio (see Eq. (15)), U is the internal energy, t is time, γ is the proportion of saturated vapor leaving or coming to the tank due to the moving boundary of saturated liquid (see Fig. 3), η_t is the expansion process efficiency for the turbine, ρ_v is density of saturated vapor, and v_l the specific volume of saturated liquid. Equations (8)–(10) represent a transient condition, and internal energy changes as long as the mass in the tank varies. Equations (11)–(14) define the compressor, expansion circuit turbine (isothermal), bypass turbines (isentropic) and cryogenic-pump power, respectively.

$$\dot{W}_c = \frac{\dot{W}_{c,iso}}{\eta_e\eta_m\eta_{c,iso}} = -\frac{\dot{m}_{liq}RT_0 ln\left(\frac{P_o}{P_i}\right)}{\eta_e\eta_m\eta_{c,iso}}, \tag{11}$$

$$\dot{W}_t = -\eta_{t,iso}\dot{W}_{t,iso} = -\eta_{t,iso}\dot{m}_{exp}RT_0 ln\left(\frac{P_o}{P_i}\right), \tag{12}$$

$$\dot{W}_{bpt} = \eta_{bpt}\dot{W}_{bpt,ie} = \eta_{bpt}z\dot{m}_{exp}(h_i - h_o), \tag{13}$$

$$\dot{W}_p = \frac{\dot{W}_{p,ie}}{\eta_p} = \frac{\dot{m}_{exp}(h_i - h_o)}{\eta_p}. \tag{14}$$

From Eqs. (11)–(14) is possible to observe that one of the mass flow rates, $\dot{m}_{exp}$ for the expansion and $\dot{m}_{liq}$ for the liquefaction, is present in all of them. Also these two rates impact the overall efficiency (see Eq. (6)): the higher the $\dot{m}_{liq}$, the greater the power consumption becomes reducing the efficiency. The opposite happens as the generated power increases with $\dot{m}_{exp}$. As long as $\dot{m}_{exp}$ and $\dot{m}_{liq}$ are independent of each other, and cause opposite effects on the efficiency, we create a dimensionless number denoted as MFR to observe this cause–effect relation:

$$MFR \equiv \frac{\text{expansion circuit mass flow rate}}{\text{liquefaction circuit mass flow rate}} = \frac{\dot{m}_{\text{exp}}}{\dot{m}_{liq}}. \tag{15}$$

For example, when MFR is less than one, $\dot{m}_{exp}$ is smaller than $\dot{m}_{liq}$, resulting in less power output and lower efficiency.

4. Results

This study is focused in a particular fluid: dry air, and the described equations were implemented using Matlab. The thermodynamic properties necessary to run the code were obtained using the toolbox CoolProp [30]. This toolbox implements the dry air expressions described in Lemmon [31] and [32] to predict basic

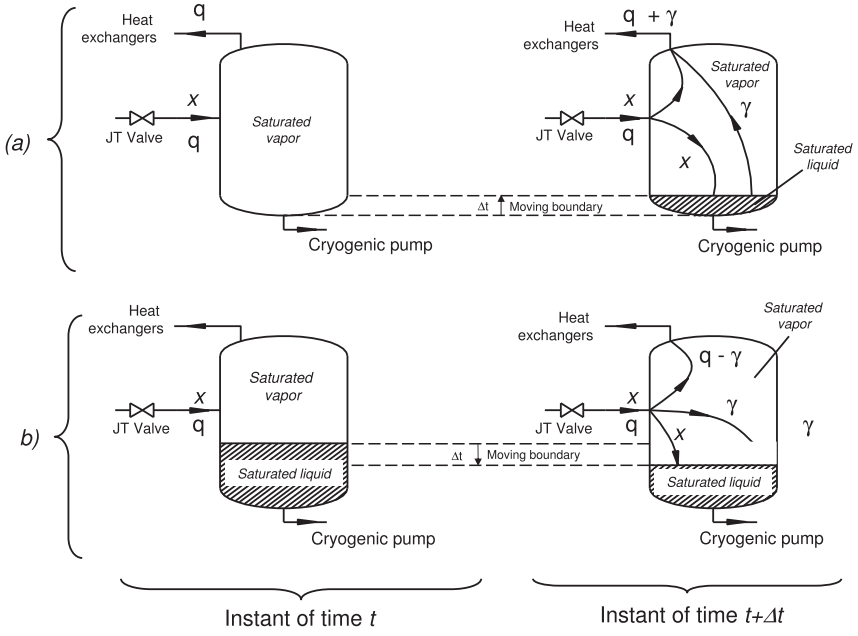

Fig. 3. Balance of mass inside the cryogenic tank, where q is proportion of saturated vapor, x the proportion of saturated liquid, and γ is the proportion of saturated air leaving or coming to the tank due the moving boundary of saturated liquid. Case (a) represents any simulation when liquid production is more than consumption, and case (b) when consumption is greater than liquid production.

Table 1
Input data used in the simulations of CES-Linde–Hampson, CES-Claude and CES-Collins.

Properties	Linde–Hampson	Claude	Collins
Absolute pressure (kPa)	101.325	101.325	101.325
Compressor inlet temp. (K)	295.15	295.15	295.15
Compressor outlet pressure (MPa)	20 [10]	4 [33]	4
Bypass Turbine 1 inlet temp. (K)	–	273.15	273.15
Bypass Turbine 2 inlet temp. (K)	–	–	263.15
z_1 Mass bypassed (Turbine 1)	–	0.75 [33]	0.56 [34]
z_2 Mass bypassed (Turbine 2)	–	–	0.16 [34]
Expansion circuit turbine inlet temp. (K)	295.15 [10]	295.15 [10]	295.15 [10]
Cryogenic pump outlet pressure (MPa)	20 [10]	20 [10]	20 [10]
Compressor efficiency	0.5985 [35]	0.5985 [35]	0.5985 [35]
Cryogenic pump efficiency	0.77 [36]	0.77 [36]	0.77 [36]
Turbine efficiency	0.88 [36]	0.88 [36]	0.88 [36]
Effectiveness	0.95	0.95	0.95

thermodynamic properties including thermal conductivity and viscosity. Table 1 lists the input values used in the simulations and the references from where they were obtained. In a real case scenario efficiency and temperatures will change according operational and ambient conditions, however those variations where not considered in this study for the sake of simplicity.

The first parameter used to compare the three CES systems is the production of saturated liquid (x). Fig. 4 shows this value as a function of *MFR* for the three CES. It shows that when *MFR* increases, the system capacity to produce liquid decreases. This is due to the fact that net production of liquid is negative for *MFR* higher than x (gray shaded area in Fig. 4) because there is more liquid being consumed than produced. As the tank empties, saturated vapor that might provide an extra cooling effect (see Fig. 3(b)) starts to contribute less ($q - \gamma$) for larger values of *MFR*, and as a consequence the net production of liquid diminishes. Saturated liquid can also start to vaporize inside the tank to maintain the mechanical equilibrium. Another important observation is that as long as the mass flow rate in the expansion and liquefaction circuits are not dependent of each other, the overall efficiency can be more than 1.0, see Eq. (6). That fact can be observed in Fig. 5 that depicts the CES efficiency for the three systems. Under 100% of efficiency (shaded area in Fig. 4) the power output is smaller than the power consumed. This region can be avoided by operating with larger values of *MFR* than the value indicated by the arrow in the same figure. The figure also shows that, in general, Collins and Claude CES systems have much larger efficiency than the simpler Linde–Hampson system. This is because the bypass turbines of Claude and Collins cycle provide part of the cooling effect needed to liquefy the air, while simultaneously generating work, whereas Linde–Hampson cycle has only a Joule–Thomson valve. Comparing the Claude and Collins systems we observe that they have similar efficiencies. Fig. 6 shows that this is in great part because they have similar power outputs, which converge to each other for larger values of *MFR*. To have a clearer perception of the *MFR* effect on the power output several values of power output and liquid production are listed in Table 2.

As all cycles were assumed to have the same expansion circuit, they present the same relative power (100%) in the expansion turbine. Differences appear due to the presence of the bypass turbines which increase the power output for the Claude and Collins systems. For example, for *MFR* = 1 the bypass turbine in the Claude

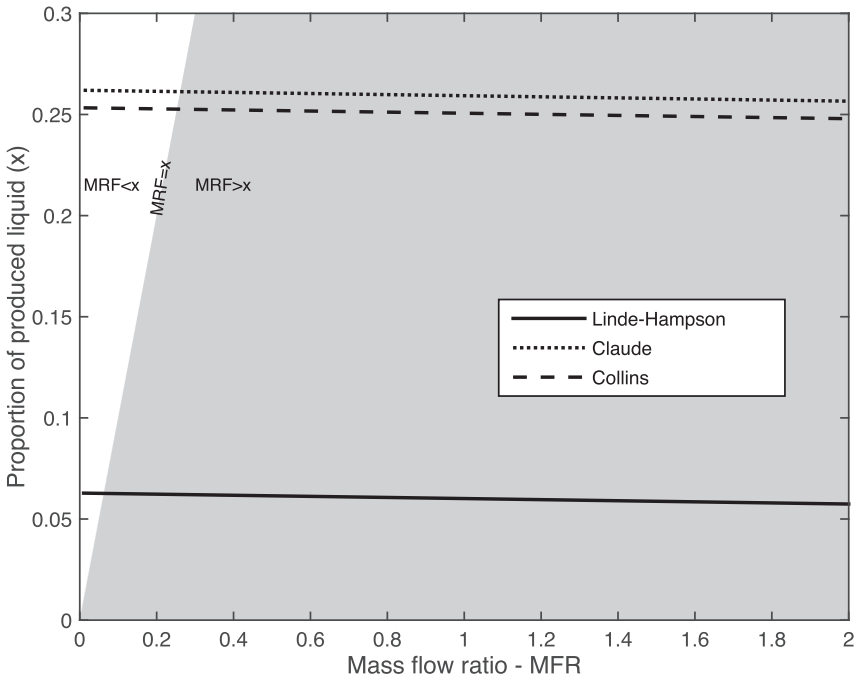

Fig. 4. Produced liquid (x) versus *MFR* for all analyzed cycles. The white and gray areas indicate positive and negative net production of liquid, respectively.

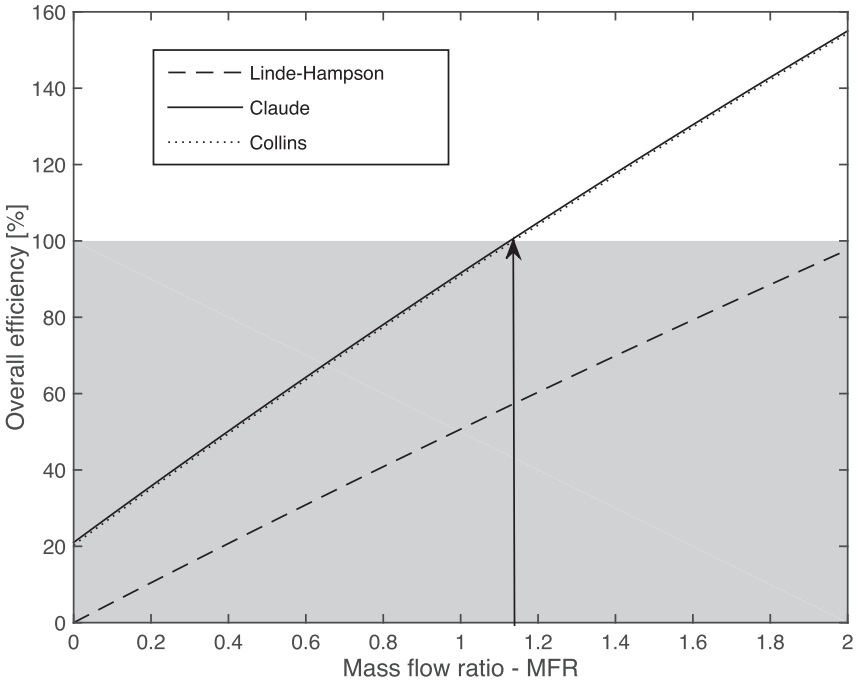

Fig. 5. Overall efficiency versus *MFR* for all combinations of CES analyzed.

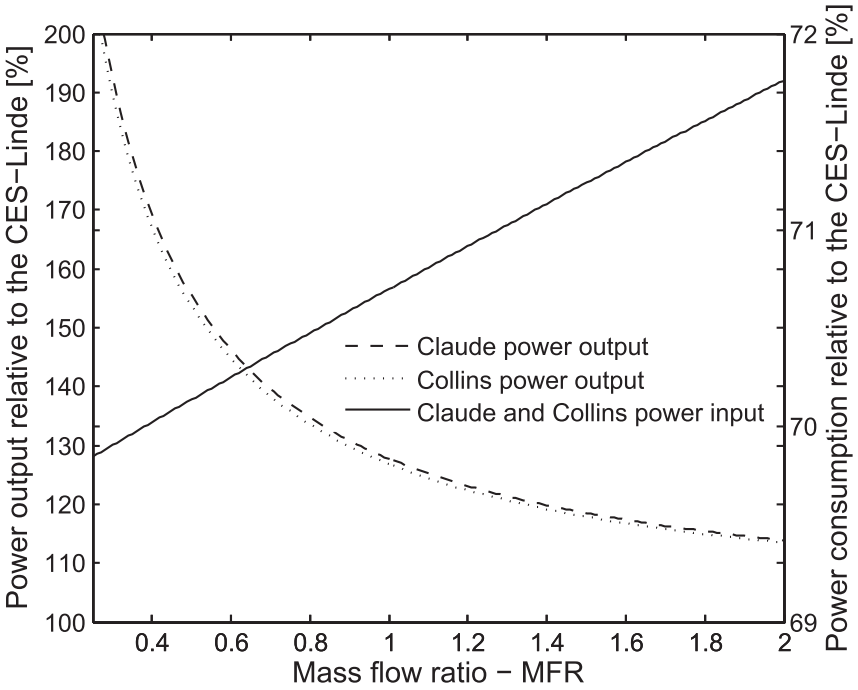

Fig. 6. Power consumption and power output as a function of *MFR* for the CES systems, relative to the CES-Linde–Hampson overall power output: $\frac{\sum \dot{W}_t}{(\dot{W}_t)_{Linde}} \times 100$.

Table 2
Contribution of the bypass turbines to increase the overall power output in the plant, relative to the CES-Linde–Hampson overall power output: $\frac{\sum \dot{W}_t}{(\dot{W}_t)_{Linde}} \times 100$.

	CES type								
	Linde–Hampson			Claude			Collins		
MFR	0.1	1	2	0.1	1	2	0.1	1	2
Power output [%]	100	100	100	377	127	113	368	126	113
Liquid yield [%]	100	100	100	418	431	446	404	417	431

system produces an additional 27% of power output relative to the expansion turbine resulting in the 127% value in Table 2. It is possible to see that the presence of the second bypass turbine in the Collins system actually reduces the power output relative to the Claude system under the conditions of this simulation (Table 1). This results from the fact that the mass flow rate for the Claude bypass turbine ($z_1 = 0.75$) is higher than the combined mass flow rates for the two bypass turbines in the Collins system

Table 3
Operational costs of compressors and turbines according to Fertig and Apt [37].

	Linde–Hampson		Claude		Collins	
	Quantity	Total $/kW	Quantity	Total $/kW	Quantity	Total $/kW
Expander	1	560	2	1120	3	1680
Compressor	1	520	1	520	1	520
Auxiliary circuits	–	216	–	328	–	440
Total	1296 $/kW		1968 $/kW		2640 $/kW	

($z_1 + z_2 = 0.72$). Also the second bypass turbine operates at a lower enthalpy difference.

The results also show that for high *MFR* Claude and Collins systems tend to have almost the same power output and liquid production. From this analysis we conclude that the second bypass turbine is unnecessary and increases costs, as shown in Table 3, which estimates the costs of the CES systems based on CAES system's costs [37]. This estimation is valid as the systems here proposed can use the similar compressor and turbine.

5. Conclusion

Currently there is much interest in energy storage systems to provide a solution to enable higher penetration of renewable sources into the power grid. In this work we evaluate various CES (cryogenic energy storage) systems that could be used for this purpose.

The simpler CES system evaluated, namely CES-Linde–Hampson, was patented by Chen et al. This is a hybrid plant comprised of liquefaction and expansion circuits working simultaneously to enhance the process' cogeneration. During the expansion process, cryogenic fluid is heated before passing through a turbine (expansion circuit) to generate electricity. Cogeneration comes from the fact that the heating source may be the air coming from the compressor (liquefaction circuit), recovering part of the cryogenic liquid spent in the expansion process, also part of the exergy, using a bypass turbines.

We propose two other alternatives to this CES system: CES-Claude and CES-Collins. We present a method to evaluate them based on energy analysis. It was concluded that CES-Claude and CES-Collins present greater efficiency, when compared to the CES-Linde–Hampson. It was also concluded that the CES-Claude and CES-Collins systems show very similar results for the power output. However, in terms of cost-benefit we conclude that the Claude system is the best option.

As a future work, optimization should be made to ensure that the tank size and discharging time will be correctly chosen, since they play an important role in the design of variable sources energy storage.

Acknowledgements

This project has been supported financially by Fapemig (Fundação de Amparo à Pesquisa do Estado de Minas Gerais) and Capes (Coordenação de Aperfeiçoamento de Pessoal de Nível Superior).

References

[1] Angelis-Dimakis A, Biberacher M, Dominguez J, Fiorese G, Gadocha S, Gnansounou E, et al. Methods and tools to evaluate the availability of renewable energy sources. Renew Sustain Energy Rev 2011;15(2):1182–200.
[2] Koroneos C, Spachos T, Moussiopoulos N. Exergy analysis of renewable energy sources. Renew Energy 2003;28(2):295–310.
[3] Rosen MA, Dincer I. Exergy as the confluence of energy, environment and sustainable development. Exergy An Int J 2001;1(1):3–13.
[4] BoroumandJazi G, Saidur R, Rismanchi B, Mekhilef S. A review on the relation between the energy and exergy efficiency analysis and the technical characteristic of the renewable energy systems. Renew Sustain Energy Rev 2012;16(5):3131–5.
[5] Hermann WA. Quantifying global exergy resources. Energy 2006;31(12):1685–702.
[6] Pleßmann G, Erdmann M, Hlusiak M, Breyer C. Global energy storage demand for a 100% renewable electricity supply. Energy Procedia 2014;46:22–31.
[7] Akhusrst M. Liquid air in the energy and transport systems. The Centre for Low Carbon Futures; 2013.
[8] Smith EM. Storage of electrical energy using supercritical liquid air. Proc Inst Mech Eng 1977:289–98.
[9] Li Y, Chen H, Zhang X, Tan C, Ding Y. Renewable energy carriers: hydrogen or liquid air/nitrogen. Appl Therm Eng 2010;30:1985–90.
[10] Chen H, Ding Y, Peters T, Berger F. A method of storing energy and a cryogenic energy storage system, US Patent, 2007.
[11] Sander M, Gehring R, Neumann H, Jordan T. LIQHYSMES storage unit and hybrid energy storage concept combining liquefied hydrogen with superconducting magnetic energy storage. Int J Hydrogen Energy 2012;37:14300–6.
[12] Li Y, Cao H, Wang S, Jin Y, Li D, Wang X, et al. Load shifting of nuclear power plants using cryogenic energy storage technology. Appl Energy 2014;113(0):1710–6.
[13] Li Y, Wang X, Jin Y, Ding Y. An integrated solar-cryogen hybrid power system. Renew Energy 2012;37(1):76–81.
[14] Zhang Q, Grossmann IE, Heuberger CF, Sundaramoorthy A, Pinto JM. Air separation with cryogenic energy storage: optimal scheduling considering electric energy and reserve markets. AIChE.
[15] Hadi K, Zadeh MRD. Real-time optimal dispatch and economic viability of cryogenic energy storage exploiting arbitrage opportunities in an electricity market. IEEE Trans Smart Grid 2015;6(1):1949–3053.
[16] Chen H, Cong TN, Yang W, Tan C, Li Y, Ding Y. Progress in electrical energy storage system: a critical review. Prog Nat Sci 2009;19(3):291–312.
[17] Li Y, Chen H, Ding Y. Fundamentals and applications of cryogen as a thermal energy carrier: a critical assessment. Int J Therm Sci 2010;49:941–9.
[18] Li Y, Jin Y, Chen H, Tan C, Ding Y. An integrated system for thermal power generation, electrical energy storage and CO_2 capture. Int J Energy Res 2011;35(13):1158–67.
[19] Deng S, Jin H, Cai R, Lin R. Novel cogeneration power system with liquefied natural gas (LNG) cryogenic exergy utilization. Energy 2004;29:497–512.
[20] Zhang N, Lior N, Liu M, Han W. {COOLCEP} (cool clean efficient power): a novel CO_2-capturing oxy-fuel power system with LNG (liquefied natural gas) coldness energy utilization. Energy 2010;35(2):1200–10.
[21] Szargut J, Szczygiel I. Utilization of the cryogenic exergy of liquid natural gas (LNG) for the production of electricity. Energy 2009;34:827–37.
[22] Bisio G, Tagliafico L. On the recovery of LNG physical exergy. In: 35th Intersociety energy conversion engineering conference & exhibit (IECEC) 1–2; 2000. p. 309–17.
[23] Bisio G, Tagliafico L. On the recovery of LNG physical exergy by means of a simple cycle or a complex system. Exergy An Int J 2002;2:34–50.
[24] Ameel B, T'Joen C, Kerpel KD, Jaeger PD, Huisseune H, Belleghem MV, et al. Thermodynamic analysis of energy storage with a liquid air Rankine Cycle. Appl Therm Eng 2013;52:130–40.
[25] Almqvist E. History of industrial gases. 1st ed. Plenum Publishers; 2002.
[26] Linde C. Process of producing low temperatures, the liquefaction of gases, and the separation of the constituents of gaseous mixtures, Patent US 727650 A 1903, 1–4.
[27] Wark K, Richards D, Richards DE. Thermodynamics. 6th ed. The McGraw-Hill Companies; 1998.
[28] Valenti G, Macchi E. Proposal of an innovative, high-efficiency, large-scale hydrogen liquefier. Int J Hydrogen Energy 2008;33(12):3116–21.
[29] Sloane TO. Liquid air and the liquefaction of gases. 2nd ed. Norman W. Henley CO; 1900.
[30] Bell IH, Wronski J, Quoilin S, Lemort V. Pure and pseudo-pure fluid thermophysical property evaluation and the open-source thermophysical property library coolprop. Ind Eng Chem Res 2014;53:2498–508.
[31] Lemmon EW, Jacobsen RT, Penoncello SG, Friend DG. Thermodynamic properties of air and mixtures of nitrogen, argon and oxygen from 60 to 2000 K air pressures to 2000 MPa. J Phys Chem 2000;29:331–85.
[32] Lemmon E, Jacobsen RT. Viscosity and thermal conductivity equations for nitrogen, oxygen, argon, and air. Int J Thermophys 2004;25:2169.

[33] Kerry FG. Industrial gas handbook: gas separation and purification. CRC Press; 2007.
[34] Kreith F. The CRC handbook of thermal engineering. 1st ed., vol. 1. Springer; 2000.
[35] Kotas TJ. The exergy method of thermal plant analysis. Exergon Publishing Company; 2012.
[36] Li Y. Cryogen based energy storage: process modelling and optimization. [Phd thesis]. University of Leeds.
[37] Fertig E, Apt J. Economics of compressed air energy storage to integrate wind power: a case study in ercot. Energy Policy 2011;39:2330–42.